IEEE Access
Multidisciplinary ⋮ Rapid Review ⋮ Open Access Journal

Received December 5, 2020, accepted December 22, 2020, date of publication December 31, 2020,
date of current version January 12, 2021.

Digital Object Identifier 10.1109/ACCESS.2020.3048499

A Fractional Brownian Motion Model for Forecasting Lost Load and Time Interval Between Power Outages

LIJIA REN[1], JUEQUAN DENG[1], WANQING SONG[1], ENRICO ZIO[2,3], (Senior Member, IEEE), AND CARLO CATTANI[4]

[1]School of Electronic and Electrical Engineering, Shanghai University of Engineering Science, Shanghai 201620, China
[2]CRC, MINES ParisTech, PSL Research University, 75006 Paris, France
[3]Department of Energy, Politecnico di Milano, 20156 Milano, Italy
[4]Engineering School (DEIM), University of Tuscia, 01100 Viterbo, Italy

Corresponding author: Lijia Ren (rlijia@126.com)

ABSTRACT A novel idea is proposed to forecast lost load and time interval between power outages based on the similarity between the series generated by a stochastic model and the actual series. The lost load obeys a power-law distribution, which can be described as a stochastic process with long-range dependence (LRD). Fractional Brownian motion (fBm) is a stochastic model with LRD, we discretize the stochastic differential equation (SDE) driven by fBm and the difference iterative equation is constructed for forecasting. By calculating the Hurst exponent of lost load series proves that it has LRD characteristics. The stochastics series produced by fBm has a strong similarity with the actual series when the Hurst exponent is taken into fBm model. Moreover, the forecasting accuracy is enriched by considering the appropriate sample size and forecasting step size. The same process for the analysis of lost load can be applied to forecast the time interval between power outages. The efficiency of the proposed model is demonstrated by a case study of the medium voltage power grid in Shanghai compared with other approaches. Finally, the value at risk (VaR) and the conditional value at risk (CVaR) as two system-level indices for assessment of future power outages.

INDEX TERMS Power outages, lost load forecasting, long-range dependence, fractional Brownian motion.

I. INTRODUCTION

Large-scale blackouts due to cascading outages are relatively rare but can lead to catastrophic consequences, with considerable social impact and serious economic loss [1]. The study of the dynamic propagation of cascading failures provides useful hints for risk management. The recent research is considering cyberattacks that may highly impact power system operation and lost load forecasting [2], [3]. Normally, the severity of cascading outages is measured in terms of lost load, to quantitatively evaluate the impact of power outages [4], [5].

The analysis of power outages and cascading events is beneficial to reveal safety operation level and mechanism of outages. This research can be achieved in two ways: one is to establish a mathematical model that specifically characterizes the process of the power outages for analysis and calculation; the other is to investigate the time series observed from the power outages based on historical events, exploring the spatio-temporal characteristic to provide information for accurately forecasting.

Recently, many mathematical models and analysis tools have been introduced, focusing on modeling the process of cascading outages and performing risk assessment [6]. Since the mechanism of cascading failures in complex networks is closely related to the cascading processes leading to blackouts in power systems, researchers are trying to analyze closely cascading failures [7]. Models of cascading failures processes based on complex network theory include topological models [8], stochastic simulation models [9], high-level statistic models [10] and so on. The calculation is mostly at elements level, with overall computational complexity that can be extremely high.

Positively, the time series analysis method does not require model assumptions nor simplifications, and the data truly reflect the situation of power outages. Little research is

The associate editor coordinating the review of this manuscript and approving it for publication was Jian Guo.

done to the data of power outages to analyze and forecast the dynamic behavior of outages from a statistical perspective [11]. Carreras *et al.* showed evidence that lost load data of power outages are consistent with self-organized criticality [12], [13], which is a model proposed to explain the origin of $1/f$ noise and fractals (self-similarity) in natural system with scale invariance and long-range dependence (LRD) characteristics in the time domain [14]. Though it is useful to do a detailed analysis of the specific causes of individual outages, it is also important to consider the global dynamic characteristics of the power transmission system, that is, the stochastic characteristics of LRD. The characteristics show that the past state of stochastic process is closely related to future state, which can offer important predictive information about the lost load series of power outages [15]. Effectively forecasting the lost load of blackouts allows performing risk evaluations of future power outages and assisting the power system operators to make operational arrangements and emergency planning by electricity reserve [16].

In power system dynamical models, exponentially accelerated model considered to generate the probability of the propagation of outages. The Markov chain is adopted to model the stochastic factors in cascading failures, which are memoryless. However, the lost load series obey a power-law distribution and has a long memory. As traditional forecasting models, such as the Neural Network, can only capture short-range dependence (SRD). The Long Short-Term Memory (LSTM) networks differ from classical Recurrent Neural Network mainly because they have ability to learn long term dependences at the cost of higher training time [17]. There is a data-driven model called long-range dependent model, the accuracy of forecasting results can be improved by taking into account the relationship between the past and future state. Two representative methods are the Fractional Auto-regressive Integrated Moving Average (FARIMA) model and the fractional Brownian motion (fBm) model. The stronger the long-term correlation of the FARIMA model, the better the performance achieved, but the higher computational complexity [18], [19]. The computational complexity of the fBm model is higher than the FARIMA model, but exhibits better forecasting performance. But the difference of computational efficiency between them would not affect the use of forecasting results in practical application. Consequently, the fBm process is more appropriate for lost load forecasting.

The fBm process has been used to model many natural phenomena since it first appeared in Mandelbrot and Van Ness [20], for instance, in hydrology [21], finance [22], [23], network traffic [24], geophysics [25], and many other domains. It is a nonstationary continuous stochastic process with stationary increments, with well-known LRD characteristics and originally proposed to describe the $1/f$ process. It can be obtained as a stochastic integral from the Brownian motion (Bm), as was already observed in [20]. The Hurst exponent [26], [27] is a key parameter of fBm, ranging from 0 to 1, which controls the regularity of the stochastic series. A special case is $H = 0.5$, the process reduces to standard Bm. The increments of fBm, often called fractional Gaussian noise (fGn), are stationary and self-similarity with parameter H. The fGn corresponds to three families of time series: for $0.5<H<1$, it exhibits positive correlation and LRD characteristics; for $0<H<0.5$, the process exhibits negative correlation and the corresponding series is of SRD; for $H = 0.5$, increments are uncorrelated.

We investigate the stochastic differential equation (SDE) driven by fBm, for which an important example is the fractional version of the Black-Scholes model proposed by Cutland, Kopp and Willinger [28]. The SDE is discretized into the difference iterative equation; then, a forecasting model is established, which fits neatly to the long memory characteristics of the process [29]. The other two parameters μ and σ in SDE dependent on the Hurst exponent, and are estimated by the maximum likelihood estimation (MLE) [30].

In practice engineering, the proposed forecasting method be used for the online application [31], [32]. The Hurst exponent of actual lost load series is calculated to identify the LRD characteristics. There are many methods to estimate the Hurst exponent. The time-domain methods are used to process the series directly, including the variance time method [33], absolute value estimation method [34] and rescaled range (R/S) method [35]. In this paper, we use the R/S method to estimate the Hurst exponent, because this method is robust to heavy tails. When $0.5<H<1$, the process exhibits positive correlation. The closer H is to 1, the greater the degree of persistence. The Hurst parameter is taken into the difference iterative equation of fBm which generates series similar with the actual series. The sample size can affect the LRD characteristics in the series. At the same time, the longer forecasting step size, the higher the error. Therefore, we choose the appropriate sample size and forecasting step size to improve the accuracy. Simulations of the lost load time series are performed by the Monte Carlo method to obtain the forecasted data. Comparisons of forecasted results with the actual lost load data show that the accuracy of forecasting is improved.

The series of time interval between power outages also carries LRD characteristics by calculating its Hurst exponent. Therefore, we use the fBm model to forecasting the time interval between power outages based on the same principle of the lost load series.Our research first developed a long-range dependent forecasting model based on fractional Brownian motion to forecast lost load and time interval between power outages.

The lost load data for theoretical analysis come from government incident reporting requirements criteria detailed in the U.S. Department of Energy (DOE) form EIA-417 in the North American Electrical Reliability Council (NERC) [36]. The criteria for a power outage include that the amount of lost load must be at least 300MW or the loss of electric service be more than 50,000 customers for one hour or more. The main causes of the power outage are severe weather and equipment failure, which shows that the past and future states of the

two major parts are closely related and correspond to LRD characteristics. The data of case study is the power outage events of the medium voltage power grid in Shanghai in 2017. The accurate results indicate the adequacy of the proposed model.

The organization of the paper is as follows. The lost load data are normalized by generation capacity as well as verified to obey a power-law distribution in Section II. Section III uses the R/S method to verify its LRD characteristics in time domain. Then, the MLE is used for parameter estimation and the fBm forecasting model is established in section IV. Section V describes the factors influencing forecasting performance, including the length of the sample size and forecasting step size, and, then, provides the procedure to select them. Case study in section VI shows the effectiveness of the proposed model to forecast lost load and time interval between power outages. Section VII analyzes the ideas of VaR and CVaR within the risk assessment of complex power outages. Finally, Section VIII concludes the paper with some remarks.

II. POWER-LAW DISTRIBUTION OF LOST LOAD

The DOE published online records which summarize the major power outage events that have occurred in North America. We analyzed 22 years of lost load data from 1996 to 2017. Fig. 1. shows the frequency of power outages in each cause category over time; the causes of large outages mainly include severe weather, equipment failure, operator error, intentional attack, supply shortage and other external causes. Severe weather and equipment failure account for a large portion of them. Fig. 2. shows the lost load time series of power outage events.

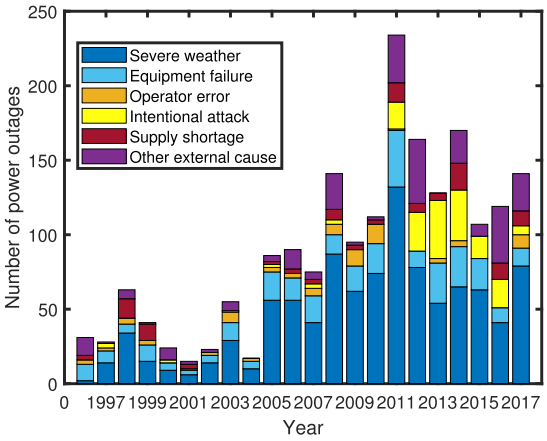

FIGURE 1. Number of power outages in each cause category over time.

In fact, the LRD properties of the power grid is mainly related to the scale of the power grid. In order to eliminate the impacts of the power grid scale [37], we normalize the lost load data by generation capacity of the year 2000, C_{2000}. The choice of year is arbitrary and it would have little effect on the results. Given the annual generation capacity data C_y,

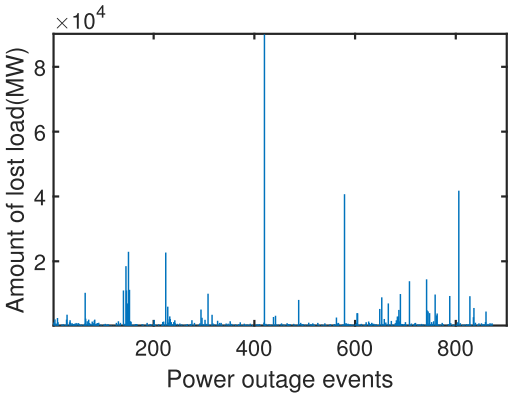

FIGURE 2. Lost load times series of power outage events (not normalized).

then

$$S_y = S\frac{C_{2000}}{C_y} \tag{1}$$

where C_{2000} is the amount of generation capacity in 2000, C_y is the amount of generation capacity in the year that need to be normalized, S is the amount of lost load before being standardized and S_y is the amount of lost load after being standardized [38]. Consequently, we standardize the data for each year separately and the diagram is shown in Fig. 3. If the probability density function (PDF) of a random variable obeys a power law distribution, it would present a straight line on the log-log plot. In many cases, it is useful to consider the complementary cumulative distribution function (CCDF) of a power law distributed variable, which we denote as $p(x) = p(X \geq x)$. We also separately analyze the Eastern and Western interconnections, and the CCDF, with power law fits in log-log plot for the distribution tails, as shown in Fig. 4. In order to distinguish the plots, North and Eastern American data are multiplied by 10^4 and 10^2, respectively. We show not the PDF but the CCDF, because the visual form of the CCDF is more robust than that of the PDF against fluctuations due to finite sample sizes, particularly in the tail of the distribution [39]. Meanwhile, we use the MLE in [40], [41] to estimate law exponent α, and Table 1 reports the values of each exponent of the power tails.

TABLE 1. power law exponents of the lost load time series.

	North America	Eastern interconnection	Western interconnection
Power law exponent α	2.1041	2.0833	2.0236

This result shows that the lost load of power outages, indeed, obeys a power-law distribution. The power-law distribution has a heavy tail characteristic, which indicates that the occurrences of large power outages are non-independent and have long memory [42]. Thus, the overall dynamic characteristics of the system should be considered when forecasting catastrophic events.

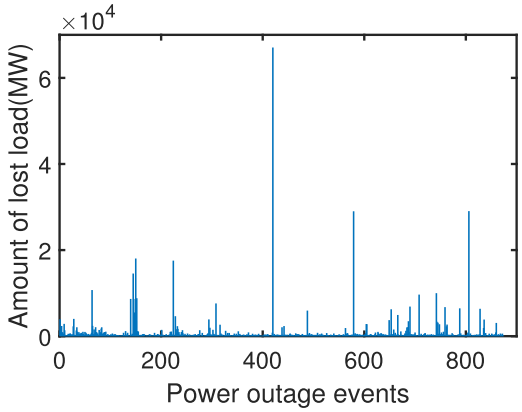

FIGURE 3. Lost load times series of power outage events (normalized).

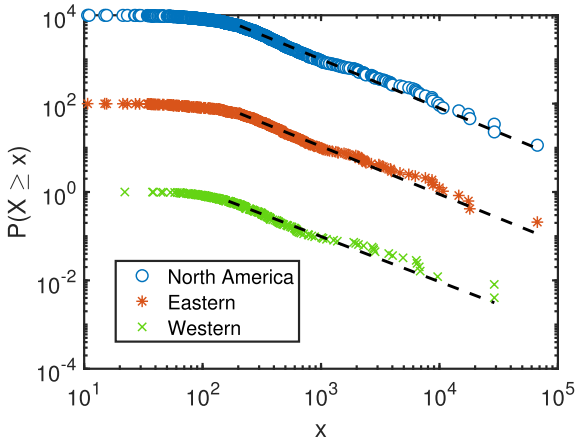

FIGURE 4. CCDF with power law fits of the lost load time series.

III. LRD CHARACTERISTICS OF THE LOST LOAD SERIES

We investigated the lost load time series of power outages from the perspective of probability distribution. Then we analyze it from the correlation function perspective. The autocorrelation function (ACF) is a measure of how similar the $x(t)$ is to itself, and it given by [43]

$$r_{xx}(\tau) = E[x(t)x(t+\tau)] = \int_{-\infty}^{\infty} x(t)x(t+\tau)p(x)dx \quad (2)$$

where $p(x)$ is PDF,τ is time lag. If $\int_{-\infty}^{\infty} r_{xx}(\tau)d\tau = \infty$, the time series $x(t)$ can be considered to have long memory [44] and the PDF follows a power-law distribution. To test if a process is exhibiting LRD properties, it is necessary to calculate its Hurst exponent, which measures the degree of self-similarity in the time series [26]:

1) When 0<H<0.5, the process exhibits negative correlation, which indicates that the time series is variable;
2) When H = 0.5, it means that the time series is randomly independent;
3) When 0.5<H<1, the process exhibits positive correlation and LRD properties. The closer H is to 1, the greater the degree of persistence.

The basic principles of the R/S analysis method are as follows: (1)

1) For a discrete time series $\{X_t : t = 1, 2, \ldots, N\}$, where N is the total number of samples, it is divided into integer sub-intervals. The mean $P(n)$ and standard deviation $S(n)$ are obtained for each sub-interval as follows, respectively:

$$P(n) = \frac{1}{n}\sum_{t=1}^{n} X_t \quad (3)$$

$$S(n) = \sqrt{\frac{1}{n-1}\sum_{t=1}^{n}(X_t - P(n))^2} \quad (4)$$

here $n(2 \le n \le N)$ is the number of observed values of each sub-interval.

2) Calculate the corresponding cumulative deviation $X(t, i)$ and range of variation $R(n)$:

$$X(t, i) = \sum_{t=1}^{n}(X_t - P(n)) \quad (5)$$

$$R(n) = \max_{1\le i\le n} X(t, i) - \min_{1\le i\le n} X(t, i) \quad (6)$$

3) Calculate the ratio of each range to the standard deviation:

$$\lg(R_s(n)) = \lg c + H \lg n \quad (7)$$

By taking different $n(2 \le n \le N)$ values, $R_s(n)$ with different interval lengths is obtained.

4) Take the logarithm n of $R_s(n)$ and the slope obtained by using least squares fitting is the Hurst parameter:

$$\lg(R_s(n)) = \lg c + H \lg n \quad (8)$$

where c is statistic constant, H is the Hurst parameter of the R/S analysis method. The R/S analysis method is used to calculate Hurst parameter of the lost load times series in NERC power outage data, and the results are shown in Fig. 5. In order to distinguish the plots, North and Western American data are translated. In addition, Table 2 shows the Hurst exponents of the lost load time series for the Eastern and Western interconnections and North America. It should be noted that the values of H obtained are actually slightly above 0.5, which indicates moderate LRD characteristics.

TABLE 2. Hurst exponents of the lost load time series.

	North America	Eastern interconnection	Western interconnection
Hurst exponent	0.5512	0.5711	0.5277

IV. THE FORECASTING MODEL OF fBm

A. CHARACTERISTIC ANALYSIS OF fBm

The fBm model whose definition is given as follows [45]. Given the Hurst parameter $H(0 < H < 1)$, the stochastic

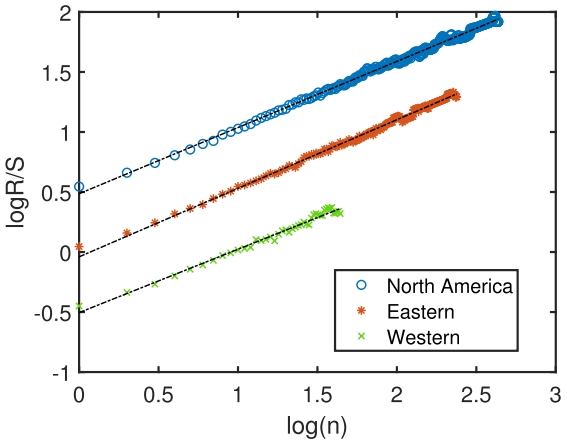

FIGURE 5. R/S analysis method to calculate the Hurst exponent of the lost load time series.

process $\left\{B_t^H, t > 0\right\}$ called fBm with Hurst parameter H, is defined as

$$B_t^H = B_0^H + \frac{1}{\Gamma(1+\alpha)} \int_{-\infty}^{t} K(t-s) dB(s) \tag{9}$$

where $\alpha = H - 0.5$, $\Gamma(1+\alpha) = \int_0^\infty x^\alpha e^{-x} dx$, $B(s)$ is Brownian motion, the integral kernel in (9) is

$$K(t-s) = \begin{cases} (t-s)^\alpha, & (0 \le s \le t) \\ (t-s)^\alpha - (-s)^\alpha, & (s < 0) \end{cases} \tag{10}$$

When $0 < H < 1$, fBm is always LRD, but this process becomes the well-known Brownian motion when $H = 0.5$. The fBm is a non-stationary process with the variance varying in time. Its ACF is given by

$$E[B_{t_1}^H B_{t_2}^H] = \frac{\sigma^2}{2} \left[{t_2}^{2H} + {t_1}^{2H} - (t_2 - t_1)^{2H} \right] \tag{11}$$

where

$$\sigma^2 = \frac{\sigma_\omega^2}{2} \frac{\cos(\pi H)}{\pi H} \Gamma(1-2H) \tag{12}$$

σ_ω^2 is a known variance. For interval $0 \le t_1 \le t_2 \le t_3 \le t_4$, the ACF of the increment process of fBm is defined as follows:

$$\begin{aligned} &E[B_{t_4}^H - B_{t_3}^H][B_{t_2}^H - B_{t_2}^H] \\ &= \frac{\sigma^2}{2} \left[(t_4 - t_1)^{2H} + (t_3 - t_2)^{2H} - (t_4 - t_2)^{2H} - (t_3 - t_1)^{2H} \right] \end{aligned} \tag{13}$$

which shows that the increment of fBm is a stationary Gaussian process. When $0.5 < H < 1$, the increments of fBm are positively correlated. The relationship between the future and past increments of fBm is determined by the Hurst exponent.

B. ESTABLISHMENT OF DIFFERENCE ITERATIVE EQUATION BASED ON fBm

In the fractional Black-Scholes model [28] for stochastic process, the SDE driven by fBm is [46], [47]:

$$dX_t = \mu X_t dt + \sigma X_t dB_t^H \tag{14}$$

From (14), it is known that the increments of fBm need to be simulated first. Extending $dB_t = \omega(t)(dt)^{\frac{1}{2}}$ of the Brownian motion proposed by Maruyama to the case of fBm and using $dB_t^H = \omega(t)(dt)^H$ to represent the increment of fBm, the SDE becomes

$$dX_t = \mu X_t dt + \sigma X_t \omega(t)(dt)^H \tag{15}$$

The time period is divided into N intervals, with time step Δt, and the discrete SDE is

$$\Delta X_t = \mu X_t \Delta t + \sigma X_t \omega(t)(\Delta t)^H \tag{16}$$

where $\Delta X_t = X_{t+1} - X_t$, $\omega(t)$is standard normal distribution. The extended formula is used to simulate the increment of fBm, which can further obtain the difference iterative equation as [48]–[50]

$$X_{t+1} = X_t + \mu X_t \Delta t + \sigma X_t \omega(t)(\Delta t)^H \tag{17}$$

Using Monte Carlo simulation, multiple approximation curves of the time series are obtained by multiple simulations, from which the approximate values at each time point can be obtained, from the most likely change path.

C. PARAMETERS ESTIMATION OF fBm

It is not enough to get the Hurst exponent and the increment Δt of fBm as there are still two unknown parameters, μ and σ. Given a certain time series, the MLE can be used to estimate the specific parameters.

The general solution of (14) can be calculated

$$X_t = X \cdot \exp(\mu t + \sigma B_t^H) \tag{18}$$

Consequently, the parameter estimation of (18) is actually equivalent to the parameter estimation of fBm with drift terms

$$Y_t = \mu t + \sigma B_t^H, t \ge 0 \tag{19}$$

We discretized the increment of fBm, thus solving the parameter estimation of the fBm model by the MLE with discrete observations. For a time series, suppose that the interval of the acquired time series is Δt, and the observation vector of $Y = (Y_0, Y_{\Delta t}, \ldots, Y_{n\Delta t})^T$ is available, with corresponding time vector $t = (0, \Delta t, \ldots, n\Delta t)^T$ for the $n+1$ observation data. The LRD series formula under fBm is derived, which makes the series formula closer to practical application. Suppose that the fBm vector is $B_t^H = \left(B_0^H, B_{\Delta t}^H, \ldots, B_{n\Delta t}^H\right)^T$, the MLE of the μ and σ in (14) can be derived from the following [30]. The joint probability density

function of the multidimensional normal distribution of Y is given as:

$$g(Y) = (2\pi\sigma^2)^{-\frac{n}{2}} \left|\Gamma_{H,i,j}\right|^{-\frac{1}{2}} \times \exp\left(-\frac{1}{2\sigma^2}(Y-\mu t)^T \Gamma_{H,i,j}^{-1}(Y-\mu t)\right) \quad (20)$$

where $\Gamma_{H,i,j} = \frac{1}{2}(\Delta t)^{2H}\left(i^{2H} + j^{2H} - |i-j|^{2H}\right)_{i,j=01,2,\ldots,n}$.

Using the joint density function to obtain the logarithmic likelihood function:

$$\ln g(Y) = -\frac{n}{2}(2\pi\sigma^2) - \frac{1}{2}\left|\Gamma_{H,i,j}\right| - \frac{1}{2\sigma^2}(Y-\mu t)^T \Gamma_{H,i,j}^{-1}(Y-\mu t) \quad (21)$$

Partial derivation of (21) with respect to μ and σ, and setting the partial derivative to zero:

$$\frac{\partial \ln g(Y)}{\partial \mu} = \frac{\partial\left(-\frac{n}{2}(2\pi\sigma^2) - \frac{1}{2}\left|\Gamma_{H,i,j}\right| - \frac{1}{2\sigma^2}(Y-\mu t)^T \Gamma_{H,i,j}^{-1}(Y-\mu t)\right)}{\partial \mu} = 0 \quad (22)$$

Because Y, t are real symmetric matrices, then:

$$t^T \Gamma_{H,i,j}^{-1} Y + Y^T \Gamma_{H,i,j}^{-1} t = (t^T Y + t Y^T)\Gamma_{H,i,j}^{-1} = 2t^T \Gamma_{H,i,j}^{-1} Y \quad (23)$$

Therefore, the MLE of $\hat{\mu}$ is:

$$\hat{\mu} = \frac{t^T \Gamma_{H,i,j}^{-1} Y}{t^T \Gamma_{H,i,j}^{-1} t} \quad (24)$$

$$\frac{\partial \ln g(Y)}{\partial \sigma^2} = \frac{\partial\left(-\frac{n}{2}(2\pi\sigma^2) - \frac{1}{2}\left|\Gamma_{H,i,j}\right| - \frac{1}{2\sigma^2}(Y-\mu t)^T \Gamma_{H,i,j}^{-1}(Y-\mu t)\right)}{\partial \sigma^2} = 0 \quad (25)$$

Then bringing (25) into $E\left[\hat{\mu}\right] = \mu$, the MLE of $\hat{\sigma}$ is:

$$\hat{\sigma}^2 = \frac{1}{n}\left[Y^T \Gamma_{H,i,j}^{-1} Y - \frac{\left(t^T \Gamma_{H,i,j}^{-1} Y\right)^2}{t^T \Gamma_{H,i,j}^{-1} t}\right] \quad (26)$$

Then, the difference iterative equation becomes

$$X_{t+1} = X_t + \hat{\mu} X_t \Delta t + \hat{\sigma} X_t \omega(t)(\Delta t)^H \quad (27)$$

The flowchart of the proposed forecasting model is presented in Fig. 6. The basic steps for the flowchart are as follows:

1) Chose lost load historical data as sample;
2) Use R/S method to calculate its Hurst exponent, it exhibits long-rang dependence characteristics when 0.5<H<1;

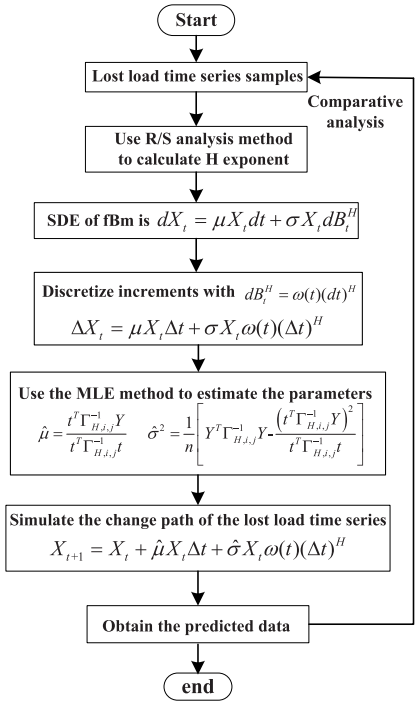

FIGURE 6. Flowchart of the fBm forecasting model.

3) Establish the difference iterative equation of fBm with discrete increments for forecasting;
4) Use the maximum likelihood estimation to estimate the parameters of the fBm model;
5) Simulate the increments to obtain the stochastic process of lost load series to obtain forecasting result compared with actual data.

V. FORECASTING ACCURACY OF THE MODEL

LRD characteristics of a series would change with different interval and forecasting performances would be considerably improved when the sample size is properly chosen. We calculate the distribution of the Hurst exponent for arbitrary interval, as shown in Table 3. The Table clearly demonstrates the randomness of the lost load time series. Specifically, in the case considered, we find that the forecasting is best when the length of sample size is within (40, 60). Actually, the lost load time series data has best LRD characteristics when the sample size is 50, which is then selected. Moreover, the longer forecasting step size, the higher the error. We notice that the

TABLE 3. Hurst exponents of the lost load time series in different intervals.

Interval	(1:874)	(10:30)	(50:100)	(100:170)
Hurst exponent	0.5512	0.4936	0.5424	0.7022
Interval	(120:300)	(250:300)	(400:600)	(510:670)
Hurst exponent	0.6818	0.4759	0.4940	0.5184
Interval	(600:670)	(670:740)	(700:800)	(800:874)
Hurst exponent	0.5643	0.5798	0.5410	0.4903

forecasting error is relatively small when the step size is 10, from Table 4.

TABLE 4. Forecasting error for different step size.

Step size	The average of max relative error (%)
10	3.35
11	3.76
12	6.05
13	7.61
14	9.32
15	11.58

With the chosen sample size and forecasting step size, forecasting has been made with the proposed model for the time series data in the years 1996-1998 of the North American electric power transmission system. Fig. 7. presents the results produced by the fBm forecasting model, compared with the actual data. Table 5 reports the forecasting errors, including max relative error (%) and mean relative error (%). The results obtained are close to the actual ones, which confirms the accuracy of forecasting.

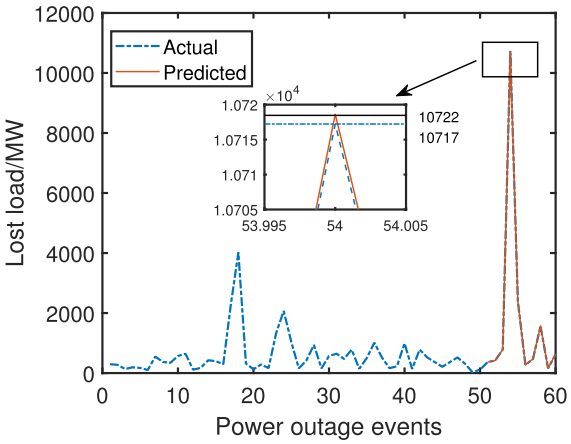

FIGURE 7. Forecasting results of lost load by the fBm model.

VI. CASE STUDY

To further evaluate the performance of our proposed forecasting model, the power outage events of medium voltage power grid in Shanghai are analyzed. The causes of these outages mainly include severe weather, equipment failure, operation management, human error, construction, transportation, animal interference and other external causes. Fig. 8. shows the frequency of outages in each cause category for every month and Fig. 9. presents the lost load time series of power outage events in 2017. Although the causes of power outages are different from those of the North American electric power transmission system, it can be seen that severe weather and equipment failure still account for a large portion. Selecting 50 as sample size and from Table 6 we can see that the forecasting error is relatively small when the forecasting step size is 10.

TABLE 5. Relative error (%) of the fBm model.

Sample	Max relative error (%)	Mean relative error (%)
1	5.20	1.21

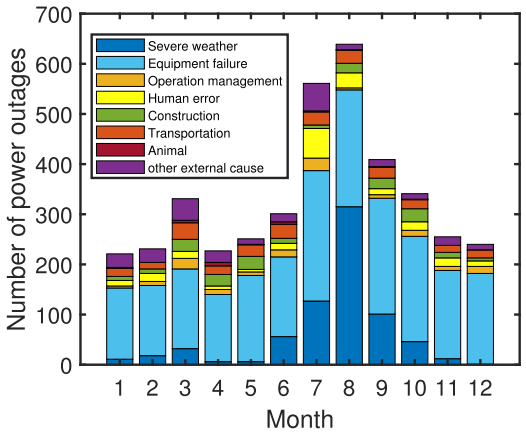

FIGURE 8. Number of power outages in each cause category over time.

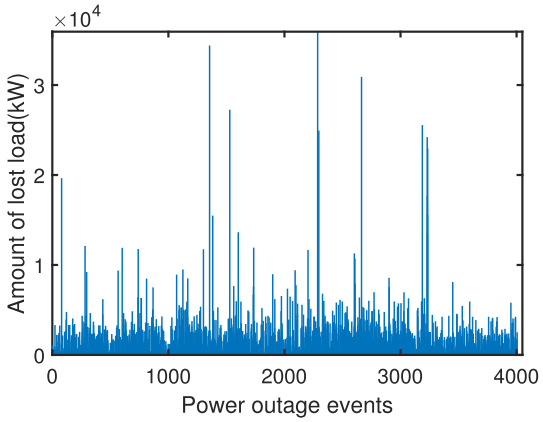

FIGURE 9. Lost load times series of power outage events.

TABLE 6. Forecasting error for different step size.

Step size	The average of max relative error (%)
10	6.17
11	6.40
12	7.03
13	8.67
14	9.99
15	11.10

An example is selected for forecasting and analysis, with the Hurst exponents given in Table 7. The lost load and time interval between power outages both follow LRD characteristics. The forecasting results of lost load by fBm model are shown in Fig. 10. Comparisons method cannot fit closely the actual lost load as shown in Fig. 11. Table 8 reports MAE (Mean Absolute Error), MAPE (Mean Absolute Percentage Error) and RMSE (Root Mean Squares Error) among them. From the results it is evident that the performance of the proposed method is better than that both of the

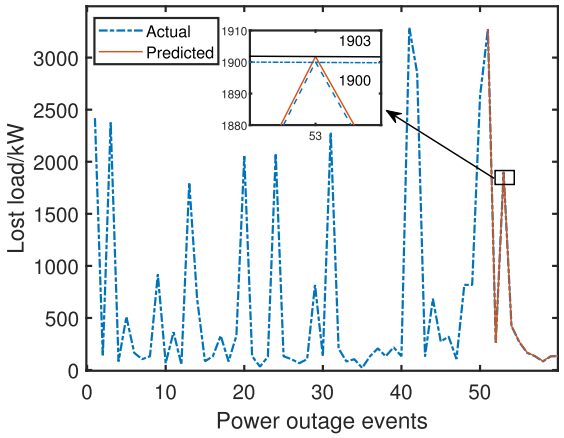

FIGURE 10. Forecasting results of lost load by fBm model.

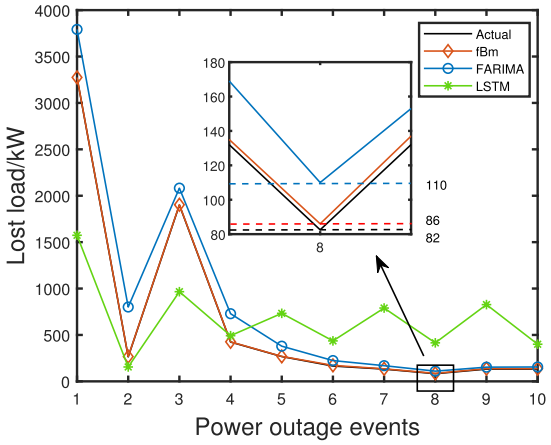

FIGURE 11. Comparisons of performance for lost load forecasting.

TABLE 7. Hurst exponents of lost load and time interval.

	Lost load	Time interval
Hurst exponent	0.5063	0.5257

TABLE 8. The evaluation indicators of different models.

Model	MAE	MAPE	RMSE
fBm	3.30	0.02	3.67
FARIMA	182	0.47	264.93
LSTM	550	2.12	718.82

FARIMA and LSTM networks. Accordingly, we use the same method to forecast the time interval between power outages. The forecasting results are quite close to the actual values are shown in Fig. 12. Furthermore, max relative error and mean relative error for both lost load and time interval are tabulated in Table 9. Although the errors of time interval larger than lost load, this is still important for power grid operators to make scheduling decisions and carry out the standby unit arrangement and commitment work.

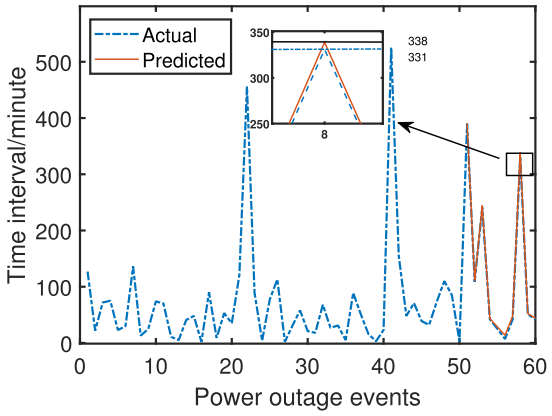

FIGURE 12. Forecasting results of time interval between power outages by the fBm model.

TABLE 9. Relative error (%)of lost load and time interval by the fBm model.

	Max relative error (%)	Mean relative error (%)
Lost load	6.81	2.06
Time interval	17.69	9.16

VII. RISK ASSEMENT

Our research provides a novel insight for performing risk assessment from the system level. In order to quantitatively characterize system-level reliability, we consider the value at risk (VaR) and conditional value at risk (CVaR) metrics for risk assessment of power outages in complex power systems [10]. The two metrics are of relatively simple calculation and easy to understand, which can accurately characterize power outage risk level with complementary characteristics. VaR accounts for the potential maximum loss that the system faces at a given confidence in a certain period of time in the future, and its definition is given by:

$$Prob(\Delta V > VaR_\theta) = 1 - \theta \tag{28}$$

where θ is the confidence, ΔV is the loss within the specified time period. For a known PDF, $p(x)$, where x represents the scale of loss and $p(x)$ is the density function of the magnitude of loss, the calculation of VaR can refer to the following formula:

$$\sigma = \int_{-\infty}^{VaR_\theta} p(x)dx \tag{29}$$

VaR combines the expected loss with the likelihood of the loss occurrence. Two limitations of VaR as a risk assessment index are that the consistency axiom is not satisfied and the insufficiency of the tail loss measurement. In order to overcome the above-mentioned shortcomings of VaR, Rockafeller and Uryasev proposed the CVaR [51], which gives the average level of excess loss. CVaR is defined as follows:

$$CVaR = \int_{VaR_\theta}^{\infty} xp(x)dx \tag{30}$$

Taking the forecasted lost load data of the medium voltage power grid in Shanghai for example, the PDF of the samples

are shown in Fig. 13. Let $\theta = 0.98$, then the VaR and CVaR are given in Table 10. From the results in the Table, taking the first sample for example, this implies that there is 98% confidence that a failure would not result in an outage size larger than 3271.5 kW of lost load. The expected value of lost load larger than 3271.5 kW is 9.69 kW. Combining these two indices, it can be seen that the system risk of the fourth sample is the largest.

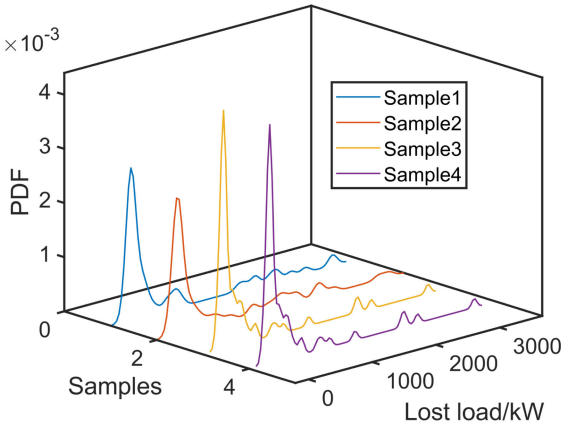

FIGURE 13. PDF of lost load with different samples.

TABLE 10. Power outage risk of samples.

Samples	VaR(kW)	CVaR(kW)
1	3271.5	9.69
2	3318.3	123.08
3	2479.6	846.57
4	4175.8	604.19

VIII. CONCLUSION

From statistical perspective, our research first time illustrated the original development of fBm forecasting model to identify the LRD characteristics and self-similarity of the lost load series and time interval between power outages. Our analysis verified LRD characteristics of lost load and time interval series, validating the proposed model considered of both the North American electric power transmission system and the medium voltage power grid of Shanghai. Comparison with other methods, the proposed modeling approach can provide accurate forecasting of lost load for a real power system to assist in the evaluation of power ouatge risk. For this, two complementary indices were used to estimate the severity of losses in future power outages, as well as to compare the reliability of different systems. Despite the accuracy of time interval between power outages is lower than lost load, it still is of great significance for power system operators to make arrangements for electricity emergency reserve and power dispatching. In the future, further research will be required to study the detailed relationship and focus on improving the forecasting accuracy of time interval between power outages. At the same time, applying the established model to more fields is also the future research direction.

REFERENCES

[1] X. Zhang, C. Zhan, and C. K. Tse, "Modeling the dynamics of cascading failures in power systems," *IEEE J. Emerg. Sel. Topics Circuits Syst.*, vol. 7, no. 2, pp. 192–204, Jun. 2017.

[2] M. G. Angle, S. Madnick, J. L. Kirtley, and S. Khan, "Identifying and anticipating cyberattacks that could cause physical damage to industrial control systems," *IEEE Power Energy Technol. Syst. J.*, vol. 6, no. 4, pp. 172–182, Dec. 2019.

[3] C. Chen, M. Cui, X. Fang, B. Ren, and Y. Chen, "Load altering attack-tolerant defense strategy for load frequency control system," *Appl. Energy*, vol. 280, Dec. 2020, Art. no. 116015.

[4] H. Guo, C. Zheng, H. H.-C. Iu, and T. Fernando, "A critical review of cascading failure analysis and modeling of power system," *Renew. Sustain. Energy Rev.*, vol. 80, pp. 9–22, Dec. 2017.

[5] M. Cui and J. Wang, "Deeply hidden moving-target-defense for cybersecure unbalanced distribution systems considering voltage stability," *IEEE Trans. Power Syst.*, early access, Oct. 15, 2020, doi: 10.1109/TPWRS.2020.3031256.

[6] M. Vaiman, K. Bell, Y. Chen, B. Chowdhury, I. Dobson, P. Hines, M. Papic, S. Miller, and P. Zhang, "Risk assessment of cascading outages: Methodologies and challenges," *IEEE Trans. Power Syst.*, vol. 27, no. 2, pp. 631–641, May 2012.

[7] C.-C. Chu and H. H.-C. Iu, "Complex networks theory for modern smart grid applications: A survey," *IEEE J. Emerg. Sel. Topics Circuits Syst.*, vol. 7, no. 2, pp. 177–191, Jun. 2017.

[8] F. Wenli, L. Zhigang, H. Ping, and M. Shengwei, "Cascading failure model in power grids using the complex network theory," *IET Gener., Transmiss. Distrib.*, vol. 10, no. 15, pp. 3940–3949, Nov. 2016.

[9] R. Yao, S. Huang, K. Sun, F. Liu, X. Zhang, S. Mei, W. Wei, and L. Ding, "Risk assessment of multi-timescale cascading outages based on Markovian tree search," *IEEE Trans. Power Syst.*, vol. 32, no. 4, pp. 2887–2900, Jul. 2017.

[10] J. Qi, I. Dobson, and S. Mei, "Towards estimating the statistics of simulated cascades of outages with branching processes," *IEEE Trans. Power Syst.*, vol. 28, no. 3, pp. 3410–3419, Aug. 2013.

[11] B. Gou, H. Zheng, W. Wu, and X. Yu, "Probability distribution of power system blackouts," in *Proc. IEEE Power Eng. Soc. Gen. Meeting*, Jun. 2007, pp. 1–8.

[12] B. A. Carreras, D. E. Newman, I. Dobson, and A. B. Poole, "Evidence for self-organized criticality in electric power system blackouts," *IEEE Trans. Circuits Syst. I, Reg. Papers*, vol. 51, no. 9, pp. 1733–1740, Sep. 2004.

[13] B. A. Carreras, D. E. Newman, and I. Dobson, "North American blackout time series statistics and implications for blackout risk," *IEEE Trans. Power Syst.*, vol. 31, no. 6, pp. 4406–4414, Nov. 2016.

[14] P. Bak, C. Tang, and K. Wiesenfeld, "Self-organized criticality: An explanation of 1/f noise," *Phys. Rev. Lett.*, vol. 59, no. 4, pp. 381–384, Aug. 1987.

[15] P. Abry, P. Borgnat, F. Ricciato, A. Scherrer, and D. Veitch, "Revisiting an old friend: On the observability of the relation between long range dependence and heavy tail," *Telecommun. Syst.*, vol. 43, nos. 3–4, pp. 147–165, Apr. 2010.

[16] O. Alizadeh Mousavi, M. Bozorg, R. Cherkaoui, and M. Paolone, "Inter-area frequency control reserve assessment regarding dynamics of cascading outages and blackouts," *Electr. Power Syst. Res.*, vol. 107, pp. 144–152, Feb. 2014.

[17] A. Sherstinsky, "Fundamentals of recurrent neural network (RNN) and long short-term memory (LSTM) network," *Phys. D, Nonlinear Phenomena*, vol. 404, Mar. 2020, Art. no. 132306.

[18] H. Sheng and Y. Chen, "FARIMA with stable innovations model of great salt lake elevation time series," *Signal Process.*, vol. 91, no. 3, pp. 553–561, Mar. 2011.

[19] C. Katris and S. Daskalaki, "Comparing forecasting approaches for Internet traffic," *Expert Syst. Appl.*, vol. 42, no. 21, pp. 8172–8183, Nov. 2015.

[20] B. B. Mandelbrot and J. W. Van Ness, "Fractional Brownian motions, fractional noises and applications," *SIAM Rev.*, vol. 10, no. 4, pp. 422–437, Oct. 1968.

[21] T. Graves, R. Gramacy, N. Watkins, and C. Franzke, "A brief history of long memory: Hurst, mandelbrot and the road to ARFIMA, 1951–1980," *Entropy*, vol. 19, no. 9, p. 437, Aug. 2017.

[22] A. N. Shiryaev, *Essentials of Stochastic Finance*. Singapore: World Scientific, 1999.

[23] L. C. G. Rogers, "Arbitrage with fractional Brownian motion," *Math. Finance*, vol. 7, no. 1, pp. 95–105, Jan. 1997.

[24] S. Stoev, M. S. Taqqu, C. Park, and J. S. Marron, "On the wavelet spectrum diagnostic for hurst parameter estimation in the analysis of Internet traffic," *Comput. Netw.*, vol. 48, no. 3, pp. 423–445, Jun. 2005.
[25] D. L. Turcotte and S. R. Brown, "Fractals and chaos in geology and geophysics," *Phys. Today*, vol. 46, no. 5, p. 68, 1993.
[26] H. E. Hurst, "Long-term storage capacity of reservoirs," *Trans. Amer. Soc. Civil Eng.*, vol. 116, no. 12, pp. 776–808, 1951.
[27] A. Shahnazi-Pour, B. P. Moghaddam, and A. Babaei, "Numerical simulation of the Hurst index of solutions of fractional stochastic dynamical systems driven by fractional Brownian motion," *J. Comput. Appl. Math.*, vol. 386, no. 113210, pp. 776–808, 2021.
[28] X.-T. Wang, W.-Y. Qiu, and F.-Y. Ren, "Option pricing of fractional version of the Black–Scholes model with Hurst exponent H being in (13,12)," *Chaos, Solitons Fractals*, vol. 12, no. 3, pp. 599–608, Jan. 2001.
[29] W. Song, C. Cattani, and C.-H. Chi, "Multifractional brownian motion and quantum-behaved particle swarm optimization for short term power load forecasting: An integrated approach," *Energy*, vol. 194, Mar. 2020, Art. no. 116847.
[30] A. Vidacs and J. T. Virtamo, "Parameter estimation of geometrically sampled fractional brownian traffic," in *Proc. IEEE Conf. Comput. Commun., 19th Annu. Joint Conf. IEEE Comput. Commun. Societies (INFOCOM)*, Mar. 2000, pp. 1791–1796.
[31] C. Opathella, A. Elkasrawy, A. A. Mohamed, and B. Venkatesh, "Optimal scheduling of merchant-owned energy storage systems with multiple ancillary services," *IEEE Open Access J. Power Energy*, vol. 7, pp. 31–40, 2020.
[32] S. Fan, G. He, X. Zhou, and M. Cui, "Online optimization for networked distributed energy resources with time-coupling constraints," *IEEE Trans. Smart Grid*, vol. 12, no. 1, pp. 251–267, Jan. 2021.
[33] M. S. Taqqu, V. Teverovsky, and W. Willinger, "Estimators for long-range dependence: An empirical study," *Fractals*, vol. 3, no. 4, pp. 785–798, Dec. 1995.
[34] A. Montanari, M. S. Taqqu, and V. Teverovsky, "Estimating long-range dependence in the presence of periodicity: An empirical study," *Math. Comput. Model.*, vol. 29, nos. 10–12, pp. 217–228, May 1999.
[35] B. B. Mandelbrot and J. R. Wallis, "Robustness of the rescaled range R/S in the measurement of noncyclic long run statistical dependence," *Water Resour. Res.*, vol. 5, no. 5, pp. 967–988, Oct. 1969.
[36] *Electric Disturbance Events Annual Summaries*. Accessed: Jun. 30, 2019. [Online]. Available: https://www.eia.gov
[37] Q. Yu, Y. Q. Qu, and L. Shi, "Self-correlation analysis of power grid blackouts based on relative value method and Hurst exponent," *Autom. Electr. Power Syst.*, vol. 42, no. 1, pp. 55–60, 2018.
[38] P. Hines, J. Apt, and S. Talukdar, "Large blackouts in north america: Historical trends and policy implications," *Energy Policy*, vol. 37, no. 12, pp. 5249–5259, Dec. 2009.
[39] S. Biswas and L. Goehring, "Load dependence of power outage statistics," *Europhys. Lett.*, vol. 126, no. 4, p. 44002, Jun. 2019.
[40] A. Clauset, C. R. Shalizi, and M. E. J. Newman, "Power-law distributions in empirical data," *SIAM Rev.*, vol. 51, no. 4, pp. 661–703, Nov. 2009.
[41] Y. Virkar and A. Clauset, "Power-law distributions in binned empirical data," *Ann. Appl. Statist.*, vol. 8, no. 1, pp. 89–119, Mar. 2014.
[42] R. V. Lenth, R. J. Alder, R. E. Feldman, and M. S. Taqqu, "A practical guide to heavy tails: Statistical techniques and applications," *J. Amer. Stat. Assoc.*, vol. 94, no. 446, p. 653, Jun. 1999.
[43] M. Li, "Fractal time series—A tutorial review," *Math. Problems Eng.*, vol. 2010, pp. 1–26, Oct. 2010.
[44] J. Beran, "Statistical methods for data with long-range dependence," *Stat. Sci.*, vol. 7, no. 4, pp. 404–416, Nov. 1992.
[45] G. Gripenberg and I. Norros, "On the prediction of fractional Brownian motion," *J. Appl. Probab.*, vol. 33, no. 2, pp. 400–410, 1996.
[46] S. J. Lin, "Stochastic analysis of fractional Brownian motions," *Stochastics An, Int. J. Probab. Stochastic Processes*, vol. 55, nos. 1–2, pp. 121–140, Nov. 1995.
[47] L. Longjin, F.-Y. Ren, and W.-Y. Qiu, "The application of fractional derivatives in stochastic models driven by fractional Brownian motion," *Phys. A, Stat. Mech. Appl.*, vol. 389, no. 21, pp. 4809–4818, Nov. 2010.
[48] G. Jumarie, "On the representation of fractional Brownian motion as an integral with respect to $(dt)^a$," *Appl. Math. Lett.*, vol. 18, no. 7, pp. 739–748, 2005.
[49] W. Song, M. Li, Y. Li, C. Cattani, and C.-H. Chi, "Fractional brownian motion: Difference iterative forecasting models," *Chaos, Solitons Fractals*, vol. 123, pp. 347–355, Jun. 2019.
[50] H. Liu, W. Song, Y. Niu, and E. Zio, "A generalized cauchy method for remaining useful life prediction of wind turbine gearboxes," *Mech. Syst. Signal Process.*, vol. 153, May 2021, Art. no. 107471.
[51] R. T. Rockafellar and S. Uryasev, "Optimization of conditional value-at-risk," *J. Risk*, vol. 2, no. 3, pp. 21–41, 2000.

LIJIA REN received the Ph.D. degree in electrical engineering from Shanghai Jiao Tong University, Shanghai, China, in 2008. She is currently with the Shanghai University of Engineering Science. Her research interests include power grid operation optimization, power system analysis, power grid planning, condition monitoring and condition maintenance of power transmission, and transformation equipment.

JUEQUAN DENG received the B.Eng. degree in electrical engineering and automation from the Institute of Technology, East China Jiaotong University, China, in 2018. She is currently pursuing the M.Eng. degree with the School of Electronic and Electrical Engineering, Shanghai University of Engineering Science, Shanghai, China. Her current research interests include reliability and economy evaluation of power systems and stability analysis of power systems.

WANQING SONG received the B.Sc. degree from the Inner Mongolia University of Science and Technology, in 1983, the M.Sc. degree from the University of Science and Technology Beijing, in 1990, and the Ph.D. degree from Donghua University, in 2010. He is currently a Professor with the Shanghai University of Engineering Science. His main research interests include condition monitor and fault diagnosis, big data analysis, health, and reliability.

ENRICO ZIO (Senior Member, IEEE) received the M.Sc. degree in nuclear engineering from the Politecnico di Milano, in 1991, the M.Sc. degree in mechanical engineering from UCLA, in 1995, the Ph.D. degree in nuclear engineering from the Politecnico di Milano, in 1996, and the Ph.D. degree in probabilistic risk assessment from MIT, in 1998. He is the author and coauthor of seven books and more than 300 articles on international journals, the Chairman and Co-Chairman of several international Conferences, an Associate Editor of several international journals, and a Referee of more than 20. His research interests include modeling of the failure-repair-maintenance behavior of components and complex systems, the analysis of their reliability, maintainability, prognostics, safety, vulnerability, resilience, and security characteristics, and the development and use of Monte Carlo simulation methods, artificial techniques, and optimization heuristics.

CARLO CATTANI is currently a Professor of Mathematical Physics with the Engineering School, Tuscia University, Italy, an Adjunct Professor with Ton Duc Thang University, Ho Chi Minh City, Vietnam, and an Honorary Professor with BSP University, Ufa, Russia. He is the author of more than 200 articles. His research interests include wavelets, fractals, fractional and stochastic equations, nonlinear waves, nonlinear dynamical systems, computational and numerical methods, data mining.